

hep-th/0008002
KIAS-P00050
IASSNS-HEP-00/57

Noncommutative Field Theory from String Theory: Two-loop Analysis

Youngjai Kiem, Sangmin Lee*

School of Physics, Korea Institute for Advanced Study, Seoul 130-012, Korea

Jaemo Park†

School of Natural Sciences, Institute for Advanced Study, Princeton, NJ 08540, USA

ABSTRACT

Noncommutative ϕ^3 field theory in six dimensions exhibits the logarithmic UV/IR mixing at the two-loop order. We show that open string theory in the presence of constant background NS-NS two-form field yields the same amplitude upon taking a decoupling limit. The stretched string picture proposed on the basis of one-loop analysis naturally generalizes to the two-loop amplitudes in consideration. Our string theory formulation can incorporate the closed string insertions as well as open string insertions. Furthermore, the analysis of the world-sheet partition function and propagators can be straightforwardly generalized to Riemann surfaces with genus zero but with an arbitrary number of boundaries.

*ykiem, sangmin@kias.re.kr

†jaemo@ias.edu

1 Introduction

Since the realization that certain noncommutative field theories are natural decoupling limits of string theory [1]-[8], there have been a number of startling discoveries on the physics in noncommutative space-time. One striking example is the UV/IR mixing in noncommutative field theory [9]; in nonplanar amplitudes of noncommutative field theories, novel IR divergences at zero momentum come from the UV regime of the loop momentum integration [10, 11]. To understand this phenomenon in the Wilsonian effective description, it was suggested that some extra (closed string) degrees of freedom might survive the decoupling limit [10].

One useful vantage point for understanding this issue is to go back to the string theory itself, and carefully examine what mechanisms are responsible for the UV/IR mixing. In this spirit, there have been attempts to recover the (nonplanar) noncommutative field theory amplitudes from the direct string theory loop calculations; indeed, at the one-loop level, one now has a fairly complete understanding of the string theory calculations [12]-[18]. The upshot is that, at the one-loop level, while one can add some extra (closed string-like or closed string-inspired) degrees of freedom to the effective action, which, upon integrating out, yield the correct IR divergence at least in the field theory analysis, it appears equally possible that the UV/IR mixing may be a purely open string phenomenon. The stretched string interpretation of [17] gives us a concrete example of the latter. Analysis of the multi-loop amplitudes should be in order.

In this paper, we develop a world-sheet approach to the noncommutative multi-loop amplitude calculation in string theory. Based on this approach, we analyze the two-loop logarithmic UV/IR mixing phenomenon in ϕ^3 field theory in six dimensions. Our calculation indicates that the stretched string interpretation advocated in [17] can be extended to the multi-loop amplitudes corresponding to nonplanar vertex insertions on planar vacuum world sheets. It remains to be seen whether the similar purely open string interpretation is possible for the nonplanar vacuum world sheet.

In section 2, we review the one and two-loop UV/IR mixing in noncommutative ϕ^3 theory in six dimensions. We recast the field theory amplitudes in a form which is straightforward to compare with the string theory calculations, following the line of investigations originating from the work of Bern and Kosower [19]-[21]. In section 3, based on the multi-loop string amplitude analysis in the absence of background NS-NS two-form field (B -field) [22]-[27], we study the modifications due to a constant background B -field. Both closed string and open string world-

sheet propagators are constructed for Riemann surfaces with boundaries (with genus zero), along with the world-sheet partition function. Using these inputs, we explicitly compute two-loop nonplanar amplitudes, which yield the two-loop amplitudes obtained in section 2 upon taking the Seiberg-Witten decoupling limit [8]. Some relevant background material and details are presented in Appendix. In section 4, we investigate the decoupling limit and the UV/IR mixing in the two-loop context.

Recently noncommutative multi-loop analysis was reported in Ref. [28] based on Reggeon vertex formalism. Our approach produces the same amplitudes as the Reggeon vertex formalism. Furthermore, it supplements that formalism in the sense that it is straightforward in our approach to consider the closed string vertex insertions, while the Reggeon vertex formalism applies only to the purely open string vertex insertions.

2 ϕ^3 Theory in $D = 6$: One and Two-loop Amplitudes

The noncommutative ϕ^3 theory in D -dimensions is described by the action

$$I = \int d^D x \left(\frac{1}{2} (\partial\phi)^2 + \frac{1}{2} m^2 \phi^2 + \frac{1}{3!} g \phi * \phi * \phi \right), \quad (2.1)$$

where the $*$ -product is defined as

$$\phi * \phi(x) = \exp \left(\frac{i}{2} \theta^{\mu\nu} \frac{\partial}{\partial y^\mu} \frac{\partial}{\partial z^\nu} \right) \phi(y) \phi(z) |_{y=z=x}. \quad (2.2)$$

We will be primarily interested in the $D = 6$ case in this paper.

At the one-loop level, the 1PI Feynman diagrams contributing to the two-point and three-point vertices shown in Fig. 1 exhibit the UV/IR mixing, the occurrence of the IR divergence from the UV corner of the momentum integral¹. For the two-point vertex, using the noncommutative Feynman rules, we have

$$V_2^{(1)}(p_1, p_2) = g^2 \delta(p_1 + p_2) W_2^{(1)}(p_1, p_2), \quad (2.3)$$

where

$$\begin{aligned} W_2^{(1)} &= \int d^D k \frac{1}{(k^2 + m^2)((k + p_1)^2 + m^2)} \exp(ik \times p_2) \\ &= \int_0^\infty dt \int_0^t d\beta t^{-D/2} e^{-m^2 t} \exp \left[p_1 \cdot p_2 \left(\beta - \frac{\beta^2}{t} \right) + p_1 \circ p_2 \frac{1}{t} \right]. \end{aligned} \quad (2.4)$$

¹Hereafter, we will neglect the overall normalization of each Feynman diagram.

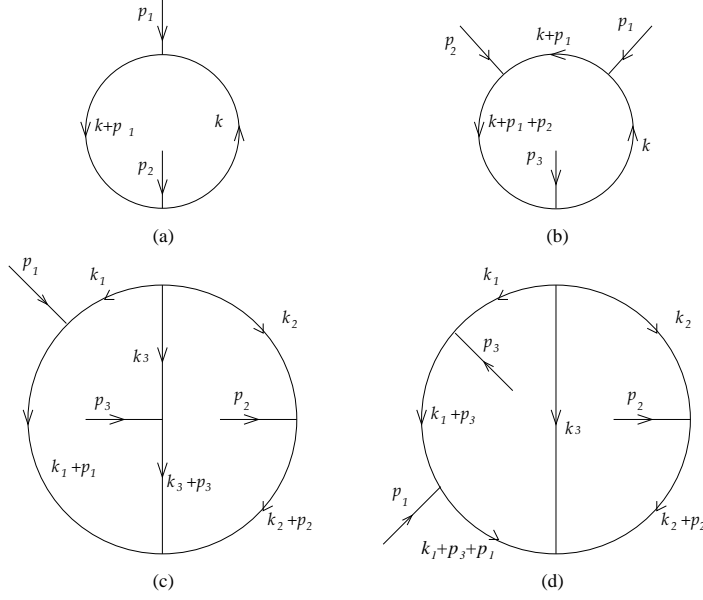


Figure 1: ϕ^3 theory Feynman diagrams.

Here the products are defined as $p_1 \cdot p_2 = p_{1\mu} p_2^\mu$, $p_1 \times p_2 = p_{1\mu} \theta^{\mu\nu} p_{2\nu}$, and $p_1 \circ p_2 = -\frac{1}{4} p_{1\mu} (\theta^2)^{\mu\nu} p_{2\nu}$ and we use the Schwinger parameterization of the internal propagators going to the second line of (2.4). To study the UV behavior ($t \rightarrow 0$) of the amplitude (2.4), we rescale the β coordinate into $\tilde{\beta} = \beta/t$ to make the integration range t -independent. We then find that as $t \rightarrow 0$, we may retain only the \circ -product term in the exponential function, resulting $W_2^{(1)} \rightarrow 1/(p_1 \circ p_1)$ in $D = 6$. This shows that (2.4) is quadratically IR divergent as the external momentum goes to zero, namely the one-loop quadratic UV/IR mixing. Similarly, the one-loop three-point vertex

$$V_3^{(1)}(p_1, p_2, p_3) = g^3 \delta(p_1 + p_2 + p_3) e^{-\frac{i}{2} p_2 \times p_3} W_3^{(1)}(p_1, p_2, p_3) \quad (2.5)$$

in Fig. 1(b) shows the logarithmic UV/IR mixing;

$$\begin{aligned}
 W_3^{(1)} &= \int d^D k \frac{1}{(k^2 + m^2)((k + p_1)^2 + m^2)((k + p_1 + p_2)^2 + m^2)} \exp(ik \times p_3) \\
 &= \int_0^\infty dt \int_0^t d\beta_1 \int_0^{\beta_1} d\beta_2 t^{-D/2} e^{-m^2 t} \exp \left[p_1 \cdot p_2 \left(\beta_1 - \beta_2 - \frac{(\beta_1 - \beta_2)^2}{t} \right) \right. \\
 &\quad \left. + p_2 \cdot p_3 \left(\beta_2 - \frac{\beta_2^2}{t} \right) + i p_2 \times p_3 \frac{\beta_2}{t} + p_2 \circ p_3 \frac{1}{t} \right. \\
 &\quad \left. + p_1 \cdot p_3 \left(\beta_1 - \frac{\beta_1^2}{t} \right) + i p_1 \times p_3 \frac{\beta_1}{t} + p_1 \circ p_3 \frac{1}{t} \right]. \quad (2.6)
 \end{aligned}$$

Rescaling the β_i coordinates by t as in (2.4) reveals that $W_3^{(1)} \rightarrow \log(p_3 \circ p_3)$ as $t \rightarrow 0$ when $D = 6$. We again note that as $t \rightarrow 0$, we may retain only the \circ -product part in the exponential function.

In this paper, we will present a full analysis of two-loop $(\text{Tr}\phi)^3$ terms in the effective action. In Ref. [28], one finds an analysis of two-loop two-point terms in the effective action. Modulo the renaming of the internal propagators and external insertions, all possible two-loop $(\text{Tr}\phi)^3$ Feynman diagrams are Figs. 1(c) and (d). We evaluate the diagram in Fig. 1(c) using the noncommutative Feynman rules and find the correction to the three-point vertex:

$$V_{3(c)}^{(2)}(p_1, p_2, p_3) = g^5 \delta(p_1 + p_2 + p_3) e^{-\frac{i}{2} p_2 \times p_3} W_{3(c)}^{(2)}(p_1, p_2, p_3), \quad (2.7)$$

where

$$W_{3(c)}^{(2)} = \int [d^D k_i] \delta(k_1 + k_2 + k_3) \exp(ik_1 \times p_3 - ik_2 \times p_2) \prod_{i=1}^3 \frac{1}{(k_i^2 + m^2)((k_i + p_i)^2 + m^2)} \quad (2.8)$$

For each internal propagator, we introduce Schwinger parameters via ($i = 1, 2, 3$)

$$\begin{aligned} \frac{1}{k_i^2 + m^2} &= \int_0^\infty d\alpha_i \exp(-(k_i^2 + m^2)\alpha_i), \\ \frac{1}{(k_i + p_i)^2 + m^2} &= \int_0^\infty d\beta_i \exp(-((k_i + p_i)^2 + m^2)\beta_i), \end{aligned}$$

and use

$$\delta(k_1 + k_2 + k_3) = \int d^D w \exp(i(k_1 + k_2 + k_3) \cdot w),$$

to rewrite (2.8) in the following form:

$$\begin{aligned} W_{3(c)}^{(2)} &= \prod_{i=1}^3 \int_0^\infty dt_i \int_0^{t_i} d\beta_i (t_1 t_2 + t_2 t_3 + t_3 t_1)^{-D/2} e^{-m^2(t_1 + t_2 + t_3)} \\ &\quad \times \exp[p_1 \cdot p_2 F_{12} + i p_1 \times p_2 G_{12} + p_1 \circ p_2 H_{12} + (\text{cyclic})]. \end{aligned} \quad (2.9)$$

Here the functions F_{12}, G_{12}, H_{12} are defined as

$$F_{12}(\beta_1, \beta_2) = \beta_1 + \beta_2 - \frac{\beta_1^2 t_2 + \beta_2^2 t_1 + (\beta_1 + \beta_2)^2 t_3}{t_1 t_2 + t_2 t_3 + t_3 t_1}, \quad (2.10)$$

$$G_{12} = \frac{\beta_1 t_2}{t_1 t_2 + t_2 t_3 + t_3 t_1}, \quad (2.11)$$

$$H_{12} = \frac{t_1 + t_3}{t_1 t_2 + t_2 t_3 + t_3 t_1}, \quad (2.12)$$

and similarly for their cyclic permutations. Going from (2.8) to (2.9), we explicitly perform the k_i - and w -integrals, introduce $t_i = \alpha_i + \beta_i$, and use the momentum conservation $p_1 + p_2 + p_3 = 0$. When the noncommutativity parameter $\theta = 0$, the amplitude (2.9) reduces to that of Ref. [20].

To examine the UV and IR limits of the amplitude, it is convenient to use a spherical polar coordinate on the t space ($t^2 \equiv t_1^2 + t_2^2 + t_3^2$ and two angles) and make a variable change $\tilde{\beta}_i = \beta_i/t_i$. This makes the integration range of β_i s be independent of t_i s. The scaling behavior of each type of term in (2.9) is readily seen to be

$$F \sim t, \quad G \sim 1, \quad H \sim t^{-1} \quad (2.13)$$

The UV limit of the amplitude (2.9) is where t goes to zero with the angles kept fixed. In that limit, (2.9) becomes

$$W_{3(c)}^{(2)} \approx \int_{S^2} d\Omega \int_{t \sim 0} dt \, t^{5-D} \exp \left[-\frac{1}{t} \left(\sum_{i=1}^3 p_i \circ p_i K_i \right) \right], \quad (2.14)$$

where K_i is defined as $K_i = t_{i+2}/(t_1 t_2 + t_2 t_3 + t_3 t_1)$ and similarly for cyclic permutations. Note that we use an identity

$$\sum_{i=1}^3 p_i \circ p_{i+1}(t_i + t_{i+2}) = - \sum_{i=1}^3 p_i \circ p_i t_{i+2}.$$

The other terms on the exponent of (2.9), including the mass term, can be neglected near $t = 0$. From (2.14), we see that there are logarithmic UV singularities when $D = 6$ if $p_1 \circ p_1 + p_2 \circ p_2 + p_3 \circ p_3 = 0$ (we recall that $p \circ p \geq 0$ for an arbitrary p)

$$W_{3(c)}^{(2)} \approx \log \left(\sum_{i=1}^3 p_i \circ p_i \right). \quad (2.15)$$

Therefore, the contributions from the UV corner of the Schwinger parameters produce the IR divergence when all the external momenta satisfy $p_a \circ p_a = 0$, the two-loop logarithmic UV/IR mixing. The potential IR divergence when $t \rightarrow \infty$ gets regulated by the mass term that scales like t in (2.9).

The 1PI amplitude of the diagram Fig. 1(d)

$$V_{3(d)}^{(2)}(p_1, p_2, p_3) = g^5 \delta(p_1 + p_2 + p_3) e^{-\frac{i}{2} p_2 \times p_3} W_{3(d)}^{(2)}(p_1, p_2, p_3), \quad (2.16)$$

where

$$\begin{aligned} W_{3(d)}^{(2)} &= \int [d^D k_i] \delta(k_1 + k_2 + k_3) \exp(ik_1 \times p_3 - ik_2 \times p_2) \\ &\times \frac{1}{\prod_{i=1}^3 (k_i^2 + m^2)((k_1 + p_3)^2 + m^2)((k_1 + p_3 + p_1)^2 + m^2)((k_2 + p_2)^2 + m^2)}, \end{aligned} \quad (2.17)$$

can also be written in a similar fashion:

$$\begin{aligned}
W_{3(d)}^{(2)} &= \prod_{i=1}^3 \int_0^\infty dt_i \int_0^{t_2} d\beta_2 \int_0^{t_1} d\beta_3 \int_0^{\beta_3} d\beta_1 (t_1 t_2 + t_2 t_3 + t_3 t_1)^{-D/2} e^{-m^2(t_1+t_2+t_3)} \\
&\times \exp \left[p_1 \cdot p_2 F_{12}(\beta_1, \beta_2) + p_2 \cdot p_3 F_{12}(\beta_3, \beta_2) + p_3 \cdot p_1 \tilde{F}_{31}(\beta_3, \beta_1) \right] \\
&\times \exp \left[i p_1 \times p_2 \frac{\beta_1 t_2 + \beta_2 t_3 + \beta_3 t_1}{t_1 t_2 + t_2 t_3 + t_3 t_1} + (p_1 \circ p_2 H_{12} + (\text{cyclic})) \right], \tag{2.18}
\end{aligned}$$

where the function \tilde{F}_{31} is defined as

$$\tilde{F}_{31}(\beta_3, \beta_1) = |\beta_3 - \beta_1| - \frac{(t_2 + t_3)(\beta_3 - \beta_1)^2}{t_1 t_2 + t_2 t_3 + t_3 t_1}, \tag{2.19}$$

and the momentum conservation implies $p_1 \times p_2 = p_2 \times p_3 = p_3 \times p_1$. A straightforward analysis shows that (2.18) is logarithmically divergent when $p_2 \circ p_2 = 0$ and it is finite otherwise.

3 Two-loop String Amplitudes

One can relate a field theory Feynman diagram to a string diagram by ‘thickening’ the lines. By thickening a l -loop planar vacuum diagram, we find that the relevant world-sheet has the topology of genus $g = 0$ and the boundary $b = l + 1$ surface, or the $(0, l + 1)$ surface if we introduce the notation (gb) to denote a surface with g handles and b boundaries. This surface can be equivalently viewed as an ‘upper half’ of the $(l0)$ surface. The boundaries are the fixed points, $w = I(w)$, under the involution I that identifies the upper and lower hemi-surfaces. Along these boundaries, we should impose an appropriate boundary condition

$$g_{\mu\nu} \partial_n X^\nu + i B_{\mu\nu} \partial_t X^\nu = 0|_{w=I(w)}, \tag{3.1}$$

where ∂_n and ∂_t are normal and tangential derivatives to the boundaries.

The main ingredients for the computation of the string theory amplitudes are the world sheet propagators and the partition function. The main goal of this section is to compute both objects for the (03) surface that corresponds to the two-loop diagrams considered in the previous section. However, most of the discussion on the world sheet partition function and the entire subsection on the world sheet propagators will be valid for a surface with arbitrary number of boundaries but no handles.

We will see that it is often convenient to use the Schottky representation for a Riemann surface. For the (03) surface, the representation is depicted in Fig. 2, where we follow the

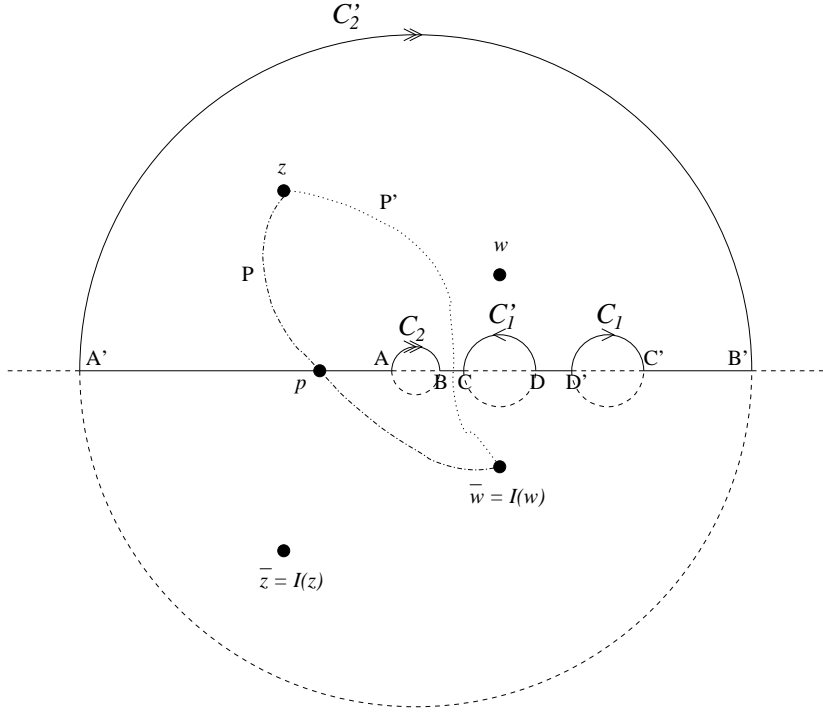


Figure 2: The (03) Surface in Schottky Representation.

conventions of Ref. [21]. Here we will only give an intuitive picture of the (03) surface; a more systematic and self-contained introduction to the Schottky representation is given in Appendix B. In Fig. 2, the (03) surface is the region in the upper half plane surrounded by the solid lines and semicircles. The involution in this representation is simply the complex conjugation, that is, $I(z) = \bar{z}$. The mirror hemi-surface under the involution is enclosed by dotted curves in the lower half plane. The two circles C_1 and C_1' are identified and similarly for the C_2 and C_2' circles. After the identification, it becomes clear that the three boundaries are $\overline{A'A}$, $\overline{BC} \cup \overline{C'B'}$ and $\overline{DD'}$

3.1 World sheet Propagator

Our strategy is to compute the closed string world sheet propagators and to extract the open string propagators from them. For this purpose, it is helpful to start from the consideration of the one-loop annulus propagators.

3.1.1 One-loop propagator revisited

Following [13] we write down the one-loop bulk propagator,

$$\begin{aligned} \langle X^\mu(z)X^\nu(z') \rangle &= \frac{\alpha'}{2}g^{\mu\nu}G(z, z') + \frac{\alpha'}{2}(2G^{\mu\nu} - g^{\mu\nu})G(z, \bar{z}') - \frac{(\theta G\theta)^{\mu\nu}}{2\pi\alpha'T}(x + x')^2 \\ &\quad + \theta^{\mu\nu} \left(\frac{1}{2\pi} \log \frac{\theta_1(z + \bar{z}'|iT)}{\theta_1(\bar{z} + z'|iT)} + \frac{2i}{T}(x + x')(y - y') \right), \end{aligned} \quad (3.2)$$

where the open string metric $G^{\mu\nu}$ and the noncommutativity parameter $\theta^{\mu\nu}$ are given in terms of the closed string variables by $G^{\mu\nu} = (g_{\mu\nu} + B_{\mu\nu})_S^{-1}$ and $\theta^{\mu\nu} = 2\pi\alpha'(g_{\mu\nu} + B_{\mu\nu})_A^{-1}$. The function $G(z, z')$ is defined as

$$G(z, z') = -\log \left| \frac{\theta_1(z - z'|iT)}{\theta_1'(0|iT)} \right|^2 + \frac{2\pi}{T}(y - y')^2, \quad (3.3)$$

The variables x and y are the real and imaginary parts of z , respectively, and T denotes the annulus modulus. The two boundaries of the world sheet are at $x = 0, 1/2$, and the propagators are periodic in $y \rightarrow y + T$.

To compute open string amplitudes, one needs a boundary propagator. Naively, one might expect to obtain the boundary propagator by taking the insertion points in (3.2) to the boundary. When $B \neq 0$, however, this procedure does not give the correct answer. To see this, we note that the quadratic terms in (3.2) as they stand do not treat the two boundaries on an equal footing. A more rigorous way to derive the boundary propagator from the bulk propagator is to use the factorization of the string *amplitudes*. When computing the amplitudes in that derivation, care should be taken to incorporate the effect of the self-contractions. In the presence of world-sheet boundaries, it is well-known that the contraction between a closed string vertex and its own mirror image should be included in such calculations². For example, the tachyon amplitude contains

$$\exp \left[- \sum_{j < i} G^{\mu\nu}(z_i, z_j) k_\mu^i k_\nu^j - \sum_i G_s^{\mu\nu}(z_i) k_\mu^i k_\nu^i \right], \quad (3.4)$$

where in the case at hand, the self-contraction is defined by

$$G_s^{\mu\nu}(z) = \frac{\alpha'}{2} \left(G^{\mu\nu} - \frac{1}{2}g^{\mu\nu} \right) G(z, \bar{z}) - \frac{2}{2\pi\alpha'T}(\theta G\theta)^{\mu\nu}x^2 \quad (3.5)$$

² The normal ordering of a closed string vertex operator is $V =: \exp(ikX(z)) :: \exp(ikX(\bar{z})) :$ in contrast to that of an open string vertex operator $V =: \exp(ik(X(z) + X(\bar{z}))) :|_{z=\bar{z}}$. When the world sheet has a boundary, $X(z)$ and $X(\bar{z})$ do not commute and produce self-contractions. At one-loop level, the operator method illustrates this aspect well. This method is useful since one does not need the knowledge of the world sheet propagator beforehand. See Appendix C for an outline of the operator method for $B \neq 0$.

As a closed string vertex operator approaches a boundary, the term involving the theta function in $G(z, \bar{z})$ becomes singular and generates the propagator for a virtual particle emitted from the boundary. On the other hand, the zero mode part remains and gets absorbed into the mutual-contractions via momentum conservation. Specifically, we make use of the following identity that holds when $\sum_i k_i = 0$.

$$\sum_{j < i} k_i \cdot k_j (x_i + x_j)^2 + 2 \sum_i k_i^2 x_i^2 = - \sum_{j < i} k_i \cdot k_j (x_i - x_j)^2. \quad (3.6)$$

It is useful to use another identity

$$\sum_{j < i} k_i \times k_j (x_i + x_j)(y_i - y_j) = - \sum_{j < i} k_i \times k_j (x_i - x_j)(y_i + y_j) \quad (3.7)$$

though it cannot be accounted for by the self-contraction. Taking these zero-mode effects into account, one obtains the planar and nonplanar boundary propagators,

$$G_P^{\mu\nu}(z, z') = \alpha' G^{\mu\nu} G(z, z') + \frac{i}{2} \theta^{\mu\nu} \epsilon(z - z'), \quad (3.8)$$

$$G_{NP}^{\mu\nu}(z, z') = \alpha' G^{\mu\nu} G(z, z') + \frac{(\theta G \theta)^{\mu\nu}}{2\pi\alpha' T} (x - x')^2 - \frac{2i}{T} \theta^{\mu\nu} (x - x')(y + y'), \quad (3.9)$$

in complete agreement with Ref. [28], where the Reggeon vertex formalism is used.

3.1.2 Multi-loop propagator

With detailed understanding of the one-loop propagators, it is now straightforward to obtain their multi-loop generalizations. The B -field background does not cause any complications except what we already encountered at one-loop.

The first step toward the generalization is to replace the theta function in (3.2) by the prime form reviewed in Appendix A. In this process, one should note that the definition of the prime form (A.9) involves the integrals $\int_{z'}^z \omega$ and $\int_{\bar{z}'}^{\bar{z}} \omega$. These integrals depend on the path of integration. To be precise, two paths give the same value for the integrals if and only if the two paths are homotopic to each other. Fig. 2 gives an example of two paths P and P' that are not homotopically equivalent. Therefore, in order for the propagator to be well-defined, we should make a specific choice of the paths.

A similar ambiguity arises for the multi-loop analogue of the quadratic part in (3.2). To see this, we define the variables $x(z)$ and $y(z)$ to be the real and imaginary part of the integral of

the Abelian differentials along a path from a reference point p to z (See Fig. 2);

$$\int_p^z \omega \equiv \Omega(z) \equiv x(z) + iy(z) , \quad (3.10)$$

where the reference point p is chosen to be an arbitrary point on the boundaries. When computing $x(z) + iy(z)$, we assume that the path from p to z lies entirely in the world-sheet and the path from p to \bar{z} , the mirror point, lies entirely in the mirror world sheet. We also demand that the paths never ‘warp’ through the pairs of circles. Using the explicit form of the Abelian differentials given in the Appendix, one can show that

$$x(z) = -x(\bar{z}), \quad y(z) = y(\bar{z}). \quad (3.11)$$

As z approach a boundary ($z = \bar{z}$), one might be tempted to say that $x(z) = x(\bar{z})$ and conclude in view of (3.11) that $x = 0$. This is true when z lies on the same boundary as the reference point p , but otherwise $x(z)$ differs from $x(\bar{z})$ by ± 1 since the difference between the two paths form a cycle homologous to one of the four circles (C_i, C'_j). In this sense, the function $x(z)$ has branch cuts along the boundaries that do not contain the reference point. We recall that the $x+x'$ term in (3.2) measures a ‘distance’ between a point and the mirror image of another point reflected along the $x = 0$ boundary (not the $x = 1/2$ one). This choice is equivalent to the choice of the reference point in our present discussion.

Using the variables x and y , we rewrite the arguments of the prime form as

$$\int_{z'}^z \omega = (x - x') + i(y - y'), \quad \int_{\bar{z}'}^z \omega = (x + x') + i(y - y'). \quad (3.12)$$

This expression together with the choices made in the definition of x and y completely fixes the ambiguity. At one loop, we observed that despite the apparent breaking of the symmetry between the two boundaries due to $(x + x')$, the correct incorporation of self-contractions restored the symmetry in the physical amplitude. In the same way, although we must choose a reference point to define the propagators, the final answer for the amplitude will not depend on the choice.

We are now ready to write down the propagators. The bulk propagator is given by

$$\begin{aligned} \langle X^\mu(z) X^\nu(z') \rangle &= \frac{\alpha'}{2} g^{\mu\nu} G(z, z') + \frac{\alpha'}{2} (2G^{\mu\nu} - g^{\mu\nu}) G(z, \bar{z}') \\ &\quad - \frac{1}{2\pi\alpha'} (\theta G \theta)^{\mu\nu} (x + x')^\alpha (T)_{\alpha\beta}^{-1} (x + x')^\beta \\ &\quad + \theta^{\mu\nu} \left(\frac{1}{2\pi} \log \frac{E(z, \bar{z}')}{(E(z, \bar{z}'))^*} + 2i(x + x')^\alpha (T)_{\alpha\beta}^{-1} (y - y')^\beta \right) , \end{aligned} \quad (3.13)$$

and the planar and nonplanar boundary propagators are

$$G_P^{\mu\nu}(z, z') = \alpha' G^{\mu\nu} G(z, z') + \frac{i}{2} \theta^{\mu\nu} \epsilon(z - z'), \quad (3.14)$$

$$G_{NP}^{\mu\nu}(z, z') = \alpha' G^{\mu\nu} G(z, z') + \frac{1}{2\pi\alpha'} (\theta G \theta)^{\mu\nu} (x - x')^\alpha (T)_{\alpha\beta}^{-1} (x - x')^\beta - 2i\theta^{\mu\nu} (x - x')^\alpha (T)_{\alpha\beta}^{-1} (y + y')^\beta, \quad (3.15)$$

where the function $G(z, z')$ is given by

$$G(z, z') = -\log |E(z, z')|^2 + 2\pi (y - y')^\alpha (T)_{\alpha\beta}^{-1} (y - y')^\beta. \quad (3.16)$$

Here the matrix T is the imaginary part of the period matrix. In fact, for the Schottky representation of the (03) surface, the period matrix is purely imaginary as explained in the Appendix. Note that the boundary propagators (3.14), (3.15) depends only on $x - x'$ that is defined unambiguously and independently of the reference point p . The value of $(y + y')$ still depends on the reference point, but the dependence drops out from the physical amplitude due to momentum conservation as we will see shortly.

3.2 World sheet partition function

In the absence of the B -field background, the partition function for the (03) surface has been known for some time [23, 24]. For N Dp-branes, the answer is given by (up to an overall normalization factor):

$$Z_{(03)} = N^3 \int dT_{11} dT_{22} dT_{12} \frac{|W(T)|}{(\det T)^{(p+1)/2}}, \quad (3.17)$$

where

$$|W(T)| = \prod_{a=1}^{10} |\theta_a(0|iT)|^{-2}.$$

Here θ_a 's are the ten even Riemann theta functions for the $g = 2$ surface.

For the one-loop (or two boundaries) partition function, an explicit computation [22] shows that the nonzero B -field background only changes the overall normalization factor. We argue here that the same should be true for arbitrary number of boundaries as long as $g = 0$.³

One may compute the partition function recursively by a gluing process. Specifically, one starts from a disk (the (01) surface) and insert two vertex operators along the boundary. By connecting these two vertex insertions and summing over all possible intermediate vertex operators,

³ After completion of this paper, we were informed that Ref. [29] gave another argument and actually computed the normalization factor for arbitrary number of boundaries.

one gets the annulus (02) partition function. Since all vertex insertions are planar, the gluing process cannot generate any non-trivial B dependence. This explains why the B -dependent factor of the annulus partition function factors out.

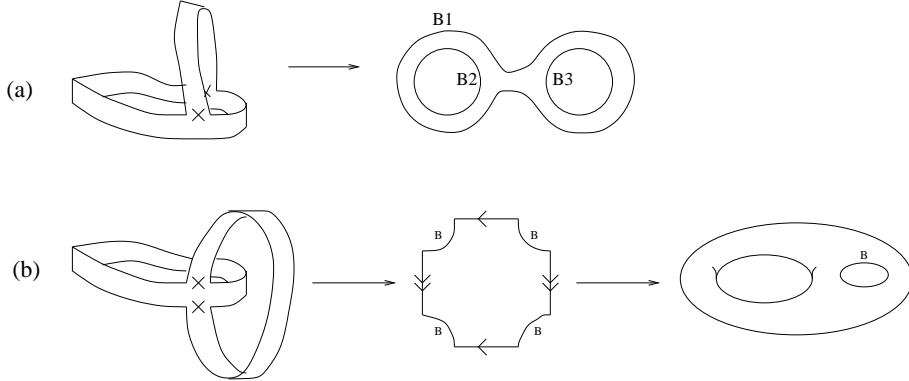


Figure 3: Getting two-loop Riemann surfaces from an annulus.

At the two-loop level, there are two possible values of g and b , giving the Euler characteristic $\chi = -1$: (11) and (03) (Fig. 3(a) and (b)). For the former partition function, we insert two vertex operators in a nonplanar fashion, connect them and sum them over all possible vertex operators. In Fig. 3(b), it is explained how this procedure produces $g = 1, b = 1$ world sheet. In this case, the propagator expression (3.15) shows that there are zero-mode contributions from the $\Theta G \Theta$ part. As a result, the partition function now contains a nontrivial Θ dependence. On the other hand, for (03), one insert two vertex operators in the planar fashion and repeat the same procedure as before. Since there are no non-trivial B -dependent (zero-mode) contributions from the propagators (as seen from (3.14)), the resulting partition function is the same as the one computed for the $B = 0$ case, up to a trivial overall multiplicative factor. By recursively adding two planar vertex insertions along the same boundary, one can show that all $g = 0, b = l + 1$ partition function is the same as the one for $B = 0$ case, modulo a trivial multiplicative factor.

3.3 The two-loop amplitudes

We are interested in the $(\text{Tr}\phi)^3$ three-point amplitudes, which are related to the field theory amplitudes in Figs. 1(c) and (d), and the string amplitudes are given by

$$\int dy_1 dy_2 dy_3 dt_1 dt_2 dt_3 \frac{|W(T)|}{(\det T)^{(p+1)/2}} \exp [-p_{1\mu} p_{2\nu} G_{NP}^{\mu\nu}(z_1, z_2) + (\text{cyclic})] . \quad (3.18)$$

Written explicitly, the world sheet nonplanar boundary propagator $G_{NP}^{\mu\nu}(z_1, z_2)$ in (3.15) becomes

$$\begin{aligned}
p_{1\mu}p_{2\nu}G_{NP}^{\mu\nu}(z_1, z_2) = & -\alpha' p_1 \cdot p_2 \log |E(z_1, z_2)|^2 \\
& + (2\pi\alpha') p_1 \cdot p_2 (y_1 - y_2)^\alpha (T)_{\alpha\beta}^{-1} (y_1 - y_2)^\beta \\
& - 2ip_1 \times p_2 (x_1 - x_2)^\alpha (T)_{\alpha\beta}^{-1} (y_1 + y_2)^\beta \\
& - \frac{4}{(2\pi\alpha')} p_1 \circ p_2 (x_1 - x_2)^\alpha (T)_{\alpha\beta}^{-1} (x_1 - x_2)^\beta ,
\end{aligned} \tag{3.19}$$

In accordance with Figs. 1(c) and (d), the insertion points are $z_3 \in A'A$, $z_1 \in BC$, and $z_2 \in DD'$ when seen in Fig. 2. We parameterize the imaginary components T of the period matrix as

$$2\pi\alpha' T = \begin{pmatrix} t_{11} & t_{12} \\ t_{12} & t_{22} \end{pmatrix} = \begin{pmatrix} t_1 + t_3 & -t_3 \\ -t_3 & t_2 + t_3 \end{pmatrix}, \tag{3.20}$$

which implies that

$$(2\pi\alpha' T)^{-1} = \frac{1}{\det(2\pi\alpha' T)} \begin{pmatrix} t_2 + t_3 & t_3 \\ t_3 & t_1 + t_3 \end{pmatrix}, \quad \det(2\pi\alpha' T) = t_1 t_2 + t_2 t_3 + t_3 t_1. \tag{3.21}$$

A direct computation in the Schottky representation gives

$$x_2 - x_1 = \begin{pmatrix} 0 \\ -1/2 \end{pmatrix}, \quad x_3 - x_2 = \begin{pmatrix} -1/2 \\ 1/2 \end{pmatrix}, \quad x_1 - x_3 = \begin{pmatrix} 1/2 \\ 0 \end{pmatrix}. \tag{3.22}$$

The quantities in (3.22) become topological for *open* string insertions; they do not change as we locally move the position of the vertex insertions, in marked contrast to the closed string insertions (see also [30]). Using (3.21) and (3.22), we find that

$$\begin{aligned}
& (2\pi\alpha') p_1 \cdot p_2 (y_1 - y_2)^\alpha (T)_{\alpha\beta}^{-1} (y_1 - y_2)^\beta + (\text{cyclic}) = \frac{(2\pi\alpha')^2 p_1 \cdot p_2}{t_1 t_2 + t_2 t_3 + t_3 t_1} \\
& \times \left[((y_1 - y_2)^2)^2 t_1 + ((y_1 - y_2)^1)^2 t_2 + ((y_1 - y_2)^1 + (y_1 - y_2)^2)^2 t_3 \right] + (\text{cyclic}),
\end{aligned} \tag{3.23}$$

$$\begin{aligned}
& 2i(p_1 \times p_2) (x_1 - x_2)^\alpha (T)_{\alpha\beta}^{-1} (y_1 + y_2)^\beta + (\text{cyclic}) \\
= & i \frac{(2\pi\alpha')(p_1 \times p_2)}{t_1 t_2 + t_2 t_3 + t_3 t_1} (t_1(y_3 - y_1)^2 + t_2(y_1 - y_2)^1 + t_3(y_3 - y_2)^1 + t_3(y_3 - y_2)^2),
\end{aligned} \tag{3.24}$$

$$\begin{aligned}
& \frac{4}{(2\pi\alpha')} p_1 \circ p_2 (x_1 - x_2)^\alpha (T)_{\alpha\beta}^{-1} (x_1 - x_2)^\beta + (\text{cyclic}) \\
= & \frac{p_1 \circ p_2(t_1 + t_3) + p_3 \circ p_1(t_2 + t_3) + p_2 \circ p_3(t_1 + t_2)}{t_1 t_2 + t_2 t_3 + t_3 t_1},
\end{aligned} \tag{3.25}$$

using $p_1 \times p_2 = p_2 \times p_3 = p_3 \times p_1$ via the momentum conservation. The expression (3.15) depends upon the combination $y + y'$, which in turn depends on a particular choice of the reference point p in Fig. 2. However, at the level of the physical amplitudes, we observe that the dependence on p drops out upon the imposition of the momentum conservation, as can be seen from the $y - y'$ dependence of (3.24).

4 Reduction from String Theory to Field Theory: Decoupling limit and UV/IR mixing

Upon taking a decoupling limit, a given string theory amplitude reproduces various field theory amplitudes represented by differing field theory Feynman diagrams, by considering appropriate corners of the moduli space. For the two-loop field theory amplitude depicted in Fig. 1(c), the reduction from the string theory amplitude has been worked out in detail in Ref. [20] in the commutative field theory setup. Following the analysis of Ref. [20], in the decoupling limit $\alpha' \rightarrow 0$, we compute

$$\begin{aligned} 2\pi\alpha'(y_2 - y_1) &= \begin{pmatrix} -\beta_1 \\ -\beta_2 \end{pmatrix}, \\ 2\pi\alpha'(y_3 - y_2) &= \begin{pmatrix} -\beta_3 \\ \beta_2 + \beta_3 \end{pmatrix}, \\ 2\pi\alpha'(y_1 - y_3) &= \begin{pmatrix} \beta_1 + \beta_3 \\ -\beta_3 \end{pmatrix} \end{aligned} \quad (4.1)$$

which relates $(y_i - y_j)$ to the field theory Schwinger parameters β_i . Following Seiberg and Witten [8], all the open string quantities, such as the open string metric $G_{\mu\nu}$ and θ , are kept fixed as we take the $\alpha' \rightarrow 0$ limit:

$$2\pi\alpha'y = \beta \rightarrow \text{fixed} \quad , \quad 2\pi\alpha'T = t \rightarrow \text{fixed} . \quad (4.2)$$

The conventions of Ref. [20] ensure that we recover the field theory propagator from the two-loop string Green function in the commutative case $\theta = 0$. In the noncommutative case, one can easily check that the θ terms (\times -product terms) and the θ^2 terms (\circ -product terms) of the field theory amplitude (2.9) is correctly reproduced from the string theory amplitude ((3.24) and (3.25), respectively); the string partition function reproduces the first line of (2.9) upon deleting the contributions from the massive string modes, and the zero mode parts of the string

propagators give the second line of (2.9), where the linear terms in β 's in (2.10) come from the zero mode parts of the generalized theta functions. In a similar fashion, to recover (2.18) depicted in Fig. 1(d) from the string theory amplitude, we compute

$$\begin{aligned} 2\pi\alpha'(y_2 - y_1) &= \begin{pmatrix} -\beta_1 \\ -\beta_2 \end{pmatrix}, \\ 2\pi\alpha'(y_3 - y_2) &= \begin{pmatrix} \beta_3 \\ \beta_2 \end{pmatrix}, \\ 2\pi\alpha'(y_1 - y_3) &= \begin{pmatrix} \beta_1 - \beta_3 \\ 0 \end{pmatrix} \end{aligned} \tag{4.3}$$

corresponding to a different corner of the moduli space, in the decoupling limit.

The outstanding issue, then, is to understand the two-loop logarithmic UV/IR mixing term (2.15) (See also (2.12), (3.25)), which originates from the $(\theta G \theta)$ part of the string propagators.

4.1 Stretched string interpretation

The stretched string interpretation of the UV/IR mixing, which does not involve the consideration of extra light (closed string) degrees of freedom was suggested in Ref. [17] at the level of one-loop analysis. When it comes to the one-loop two-point nonplanar amplitudes, we insert vertex operators along each of the two boundaries of an annulus. The analog UV/IR mixing term in this context is

$$\frac{1}{2\pi\alpha' T} p \circ p \tag{4.4}$$

where p is the external momentum.

Even in the decoupling limit $\alpha' \rightarrow 0$, (4.4) remains finite (recall (4.2)); it essentially corresponds to the length squared of a rigid, nondynamical ‘stretched string,’ whose length $\Delta X^\mu = \theta^{\mu\nu} p_\nu$ corresponds to the short-distance cutoff introduced by the noncommutativity parameter θ . The ‘size’ of the Feynman diagram cannot shrink below the length scale ΔX set by the stretched string, and this fact reflects the inherent nonlocality of a noncommutative theory.

As seen from (4.4), the way a stretched string contribution enters into the amplitudes is formally similar to the ($s \rightarrow 1/t$ modular transformed) contribution from the winding modes of closed strings (see also Refs. [31, 32, 33]). Comparing (4.4) with its two loop counterparts (3.25), we observe that the stretched string interpretation of Ref. [17] naturally carries over to the multi-loop amplitudes, which result from the nonplanar vertex insertions on a *planar* vacuum world sheet. In fact, more subtle types of amplitudes are those resulting from a *nonplanar*

vacuum world sheet, which necessarily has a positive genus. For these kinds of amplitudes, there are integrations over the momenta appearing in $(p \circ p)$. As a result, the stretching length $\theta^{\mu\nu} p_\nu$ can be larger or smaller than the string length $\sqrt{\alpha'}$ depending on the value of the loop momentum p_ν . In contrast, the winding (closed) strings have a fixed space-time size. Taking the decoupling limit in this case necessarily involves more careful analysis of the competition between the two length scales.

Acknowledgements

Y. K. would like to thank the high energy theory group of Princeton University for the hospitality during his visit. We are grateful to C.-S. Chu for valuable discussions.

Appendix

A A Brief Review of Riemann Surfaces

For a genus g Riemann surface Σ_g , we choose $2g$ linearly independent cycles a_α, b_α ($\alpha = 1, \dots, g$) such that the intersection pairings satisfy

$$(a_\alpha, a_\beta) = (b_\alpha, b_\beta) = 0, \quad (a_\alpha, b_\beta) = -(b_\alpha, a_\beta) = \delta_{\alpha\beta}. \quad (\text{A.1})$$

Any such basis is called *canonical*. We can also find g linearly independent holomorphic closed one-forms ω_α and their complex conjugates $\bar{\omega}_\alpha$ called *Abelian differentials*. We normalize the ω_α 's along the a -cycles, then the periods over the b -cycles give the *period matrix*;

$$\int_{a_\alpha} \omega_\beta = \delta_{\alpha\beta}, \quad \int_{b_\alpha} \omega_\beta = \tau_{\alpha\beta}. \quad (\text{A.2})$$

The period matrix is symmetric and its imaginary part is positive definite.

Consider a mapping between two canonical bases of the same Riemann surface,

$$\begin{pmatrix} a' \\ b' \end{pmatrix} = M \begin{pmatrix} a \\ b \end{pmatrix} = \begin{pmatrix} D & C \\ B & A \end{pmatrix} \begin{pmatrix} a \\ b \end{pmatrix}, \quad (\text{A.3})$$

where M is a $2g \times 2g$ matrix composed of the $g \times g$ blocks A, B, C, D . To preserve the intersection pairing (A.1), the matrix M must satisfy

$$M J M^T = J, \quad J = \begin{pmatrix} 0 & 1 \\ -1 & 0 \end{pmatrix}, \quad (\text{A.4})$$

that is, $M \in Sp(2g, \mathbb{Z})$. Normalizing the Abelian form in the new basis, we find a relation between the period matrices in the two bases:

$$\tau' = (A\tau + B)(C\tau + D)^{-1}. \quad (\text{A.5})$$

The integral of the Abelian differentials along a path on the Riemann surface $\Omega_\alpha = \int \omega_\alpha$ naturally introduces a lattice in \mathbb{C}^g . The *Riemann theta functions* are defined on \mathbb{C}^g to be the sum of Gaussian functions over the lattice,

$$\theta \left[\begin{smallmatrix} \alpha \\ \beta \end{smallmatrix} \right] (z|\tau) = \sum_{n \in \mathbb{Z}^g} \exp 2\pi i \left[\frac{1}{2}(n + \alpha)\tau(n + \alpha) + (n + \alpha)(z + \beta) \right], \quad (\text{A.6})$$

where $2\alpha, 2\beta \in \mathbb{Z}^g$ and $z \in \mathbb{C}^g$. It follows from the definition that

$$\begin{aligned} \theta \left[\begin{smallmatrix} \alpha \\ \beta \end{smallmatrix} \right] (z + m_1 + \tau m_2 | \tau) &= \exp 2\pi i \left[-\frac{1}{2}m_2\tau m_2 - m_2 z + m_1\alpha - m_2\beta \right] \theta \left[\begin{smallmatrix} \alpha \\ \beta \end{smallmatrix} \right] (z | \tau) \\ \theta \left[\begin{smallmatrix} \alpha \\ \beta \end{smallmatrix} \right] (-z | \tau) &= \exp [4\pi i \alpha \beta] \theta \left[\begin{smallmatrix} \alpha \\ \beta \end{smallmatrix} \right] (z | \tau). \end{aligned} \quad (\text{A.7})$$

Using the second relation, one can show that among the 2^{2g} theta functions, $2^{g-1}(2^g + 1)$ are even and $2^{g-1}(2^g - 1)$ are odd.

The *prime form* is a $(-1/2, -1/2)$ form defined on $\Sigma_g \otimes \Sigma_g$ by

$$E(z, w|\tau) = \frac{\theta \left[\begin{smallmatrix} \alpha \\ \beta \end{smallmatrix} \right] (\int_w^z \omega|\tau)}{\sqrt{\partial_\alpha \theta(0|\tau) \omega_\alpha(z)} \sqrt{\partial_\beta \theta(0|\tau) \omega_\beta(w)}}. \quad (\text{A.9})$$

Here z and w are coordinates on Σ_g and the theta function can be any one of the odd theta functions. Note that when z approaches w , $E(z, w) \sim (z - w)/\sqrt{dz}\sqrt{dw}$. By slight abuse of notation, we sometimes write $E(z, w)$ in place of $E(z, w)\sqrt{dz}\sqrt{dw}$. The transformation rule for the prime form follows from that of the theta function; for a fixed value of w , the prime form remains unchanged when z moves around an a -cycle, while it changes by

$$E(b_k(z), w) = -\exp \left[-2\pi i \left(\frac{1}{2} \tau_{kk} + \int_w^z \omega_k \right) \right] E(z, w), \quad (\text{A.10})$$

when z moves around a b -cycle.

The world sheet of an open string theory is a Riemann surface with boundary. An efficient way to describe such a surface is to begin with a surface Σ without boundary and “folding” it by an involution. The involution I is an orientation-reversing diffeomorphism from Σ onto itself. The set of fixed points of I becomes the boundary of the resulting surface.

Clearly, the involution preserves the intersection pairing, but changes its sign. Therefore,

$$\begin{pmatrix} a' \\ b' \end{pmatrix} = I \begin{pmatrix} a \\ b \end{pmatrix} = \begin{pmatrix} H & G \\ F & E \end{pmatrix} \begin{pmatrix} a \\ b \end{pmatrix} \Rightarrow IJI^T = -J. \quad (\text{A.11})$$

If the complex structure on the covering space Σ is compatible with the involution, holomorphic differential forms are mapped to antiholomorphic ones and vice versa. The compatibility condition gives a constraint on the period matrix. Note that any integral of a closed form over a homology cycle is invariant under the involution. In particular,

$$\int_{I_*(a_\alpha)} I^*(\omega_\beta) = \delta_{\alpha\beta}, \quad \int_{I_*(b_\alpha)} I^*(\omega_\beta) = \tau_{\alpha\beta}. \quad (\text{A.12})$$

It follows that

$$\tau = (E\bar{\tau} + F)(G\bar{\tau} + H)^{-1}. \quad (\text{A.13})$$

B A Brief Review of Schottky Representation

B.1 Generality

This subsection is based on Appendix A of [34]. Via stereographic projection, a two sphere can be represented as the complex plane with a point at infinity added ($S^2 = \mathbb{C} \cup \{\infty\}$). One may attach a handle to the sphere by removing a pair of discs with equal radii from $\mathbb{C} \cup \{\infty\}$ and identifying the two boundaries with opposite orientation. Repeating this procedure g times, one obtains a genus g Riemann surface.

The Schottky representation realizes this idea quantitatively. One begins with g independent projective transformations $P_\alpha \in SL(2, \mathbb{C})$, which act on $\mathbb{C} \cup \{\infty\}$ in the usual way. The Schottky group \mathcal{G}_g is the group generated by the P_α 's. For our purposes, it is convenient to specify the generators by their fixed points η_α, ξ_α and multipliers k_α defined implicitly by

$$\frac{P_\alpha(z) - \eta_\alpha}{P_\alpha(z) - \xi_\alpha} = k_\alpha \frac{z - \eta_\alpha}{z - \xi_\alpha} \quad (\text{B.1})$$

The two discs D_α, D'_α associated to each P_α are defined by

$$D_\alpha : \left| \frac{dP_\alpha}{dz} \right|^{-1/2} \leq 1, \quad D'_\alpha : \left| \frac{dP_\alpha^{-1}}{dz} \right|^{-1/2} \leq 1. \quad (\text{B.2})$$

Let the circles C_α and C'_α be the boundary of the discs. It is straightforward to show that the radii R_α, R'_α and the centers J_α, J'_α of the circles are given by

$$R_\alpha = R'_\alpha = \sqrt{|k_\alpha|} \frac{|\xi_\alpha - \eta_\alpha|}{|1 - k_\alpha|}, \quad J_\alpha = \frac{\xi_\alpha - k_\alpha \eta_\alpha}{1 - k_\alpha}, \quad J'_\alpha = \frac{\eta_\alpha - k_\alpha \xi_\alpha}{1 - k_\alpha}. \quad (\text{B.3})$$

It can be shown that P_α maps D_α onto $(\mathbb{C} \cup \{\infty\} - D'_\alpha)$ and similarly for P_α^{-1} . A bit of thought shows that the fundamental region of the Schottky group is precisely the region exterior to all the discs, or the Riemann surface we had in mind.

$$\Sigma_g = \mathbb{C} \cup \{\infty\} - \cup_{\alpha=1}^g (D_\alpha \cup D'_\alpha) \quad (\text{B.4})$$

A Schottky representation has a preferred choice of canonical basis; the a_α cycle corresponds to the circle C_α or C'_α , while the b_α cycle corresponds to a path from a point on C_α to its image by P_α on C'_α .

The Abelian differentials and the prime form in a Schottky representation are given by

$$\omega_\alpha = \sum_a \left(\frac{1}{z - T_a(\eta_\alpha)} - \frac{1}{z - T_a(\xi_\alpha)} \right) \frac{dz}{2\pi i}, \quad (\text{B.5})$$

$$E(z, w) = \frac{z - w}{\sqrt{dz} \sqrt{dw}} \prod_a \frac{z - T_a(w)}{z - T_a(z)} \frac{w - T_a(z)}{w - T_a(w)}, \quad (\text{B.6})$$

where the summation index runs over all the elements $\{T_a\}$ of the Schottky group except for the elements having P_α as the right-most factor, and the product index runs over all elements except for the identity (furthermore, T_a and T_a^{-1} are counted only once).

The Abelian differentials ω_α apparently have poles at $T_a(\eta_\alpha)$ and $T_a(\xi_\alpha)$. All the poles in fact lie inside the discs, and therefore ω_α are holomorphic in the entire Riemann surface Σ_g . Next, when one integrates ω_α along an a_β cycle, or the circle C_β , each pole in the sum (B.5) contribute ± 1 . It is easy to show that they cancel pair-wise except when T_a is the identity element, so that the normalization condition (A.2) is satisfied.

Although the expression for the prime form given in (B.6) look quite different from its definition (A.9), they can be shown to have the same analytic and periodic properties, hence they should be equal.

B.2 The (03) surface

Clearly, the $g = 0, b = 3$ surface is obtained by folding the $g = 2, b = 0$ surface. The Schottky representation of the (03) surface is obtained from that of the (20) surface in the following way. First, place the centers of the circles along the real axis such that C_1 is adjacent to C'_1 and C_2 to C'_2 . Then take the involution to be the complex conjugation on $\mathbb{C} \cup \{\infty\}$.

We may use the $SL(2, \mathbb{R})$ invariance of the upper half plane to fix three of the six parameters that define the generators of the Schottky group. Following [21], we choose $\eta_2 = 0, \xi_2 \rightarrow \infty$ and $\xi_1 = 1$. Without loss of generality, we can also let η_1 move between 0 and 1. Using (B.3), we find that the radii and the centers of the circles in Fig. 2 are

$$R_1 = R'_1 = \sqrt{k_1} \frac{1 - \eta_1}{1 - k_1}, \quad J_1 = \frac{1 - k_1 \eta_1}{1 - k_1}, \quad J'_1 = \frac{\eta_1 - k_1}{1 - k_1}, \quad (\text{B.7})$$

$$R_2 = R_2'^{-1} = \sqrt{k_2}, \quad J_2 = J'_2 = 0. \quad (\text{B.8})$$

Note that not only the fixed points but also their images under the elements of the Schottky group lie on the real axis. This fact has three consequences. First, it follows from (B.5) that the period matrix is purely imaginary. It is consistent with (A.13) since in the case at hand $E = -H = 1, F = G = 0$. Next, we see again from (B.5) that

$$\omega_\alpha/dz + \text{c.c.} = 0|_{z=\bar{z}}. \quad (\text{B.9})$$

Finally, eq. (B.6) shows that

$$\overline{E(z, w)} = E(\bar{z}, \bar{w}) \quad (\text{B.10})$$

C World-Sheet Propagators

C.1 Operator method at one-loop for $B \neq 0$

For simplicity, we consider the case $B_{12} = B$ and $B_{\mu\nu} = 0$ otherwise. The mode expansion of the $X = (X^1, X^2)$ is given by

$$X(\tau, \sigma) = RX(\tau + \sigma) + R^T X(\tau - \sigma), \quad (\text{C.1})$$

where the mode expansion for the right-mover and the left-mover are given by

$$X(\tau + \sigma) = \frac{1}{2}x + \alpha' p(\tau + \sigma - \pi/2) + i\sqrt{\frac{\alpha'}{2}} \sum_{n \neq 0} \frac{\alpha_n}{n} e^{-in(\tau+\sigma)} \quad (\text{C.2})$$

$$X(\tau - \sigma) = \frac{1}{2}x + \alpha' p(\tau - \sigma + \pi/2) + i\sqrt{\frac{\alpha'}{2}} \sum_{n \neq 0} \frac{\alpha_n}{n} e^{-in(\tau-\sigma)}. \quad (\text{C.3})$$

and as in Ref. [35], we introduced the rotation matrix,

$$R = \begin{pmatrix} \cos \phi & \sin \phi \\ -\sin \phi & \cos \phi \end{pmatrix}, \quad \tan \phi = B. \quad (\text{C.4})$$

The effect of the B field is completely summarized by the rotation matrix, and the commutation relations of the modes in (C.2), (C.3) are exactly the standard ones. The variables (σ, τ) are related to the (x, y) in Section 3.2 by $2\pi(x, y) = (\sigma, \tau)$. The $\pm\pi/2$ shifts in the linear terms of (C.2), (C.3) are to ensure that the same magnitude of noncommutativity is measured at the two boundaries.

Given the mode expansion, the computation of scattering amplitudes in the operator method is straightforward. When all the external particles are open string states, the details are given in Ref. [36]. For closed string insertions, the only subtlety is that when one writes down vertex operators, one should take the normal ordering for the left-mover and the right-mover separately,

$$V(\tau, \sigma) = :e^{ikRX(\tau+\sigma)}: :e^{ikR^T X(\tau-\sigma)}: . \quad (\text{C.5})$$

C.2 Analysis of the multi-loop bulk propagator

In this subsection, we show the validity of the world-sheet propagator given in Section 3.2. It suffices to consider a simple case when the only nonzero component of the B -field is $B_{12} = B$

and $g_{\mu\nu} = \delta_{\mu\nu}$, the propagators for $X = X^1$ and $Y = X^2$ reduce to

$$\langle X(z)X(z') \rangle = G(z, z') + \frac{1-B^2}{1+B^2} G(z, \bar{z}') + \frac{4\pi B^2}{1+B^2} (T)_{\alpha\beta}^{-1} (x+x')^\alpha (x+x')^\beta, \quad (\text{C.6})$$

$$\langle Y(z)X(z') \rangle = \frac{2B}{1+B^2} \left(\log \frac{E(z, \bar{z}')}{(E(z, \bar{z}'))^*} + 4\pi i (T^{-1})_{\alpha\beta} (x+x')^\alpha (y-y')^\beta \right). \quad (\text{C.7})$$

Let us first check the periodicity of the $\langle XX \rangle$ propagator in (C.6). Note that under a periodic shift along the b_γ -cycles, the quadratic term in G changes by

$$\Delta \{ 2\pi (T)_{\alpha\beta}^{-1} (y_1 - y_2)^\alpha (y_1 - y_2)^\beta \} = 4\pi (y_1 - y_2)^\gamma + 2\pi T_{\gamma\gamma} = 4\pi \text{Im} \int_{z_2}^{z_1} \omega_\gamma + 2\pi T_{\gamma\gamma}. \quad (\text{C.8})$$

These two additional pieces precisely cancel the pieces coming from the transformation of the prime form in (A.10), making G invariant. Note that the a_k -cycles are no longer cycles along which the periodicity should be required, since they are odd under the involution. Since the real part of the period matrix is zero, the quadratic piece in $\langle XX \rangle$ remains invariant under the b_k -cycle shift.

For the $\langle XY \rangle$ propagators (C.7), the periodic shift along the b_γ -cycle changes its quadratic pieces as

$$\begin{aligned} & 4\pi i (T^{-1})_{\alpha\beta} (x+x')^\alpha (y-y')^\beta \\ \rightarrow & 4\pi i (T^{-1})_{\alpha\beta} (x+x')^\alpha (y-y')^\beta + 4\pi i (x+x')^\gamma \end{aligned} \quad (\text{C.9})$$

for the period matrix is purely imaginary. The extra piece from (C.9) is precisely what cancels the extra piece from the transformation of the prime form (A.10), making $\langle XY \rangle$ periodic.

To check the boundary condition, it is easiest to use the Schottky representation of the previous section. The boundary condition reads

$$(\partial - \bar{\partial}) \langle X(z)X(w) \rangle - B(\partial + \bar{\partial}) \langle Y(z)X(w) \rangle = 0|_{z=\bar{z}}, \quad (\text{C.10})$$

where the derivatives act on z only. Using (B.10), one can easily show that the terms involving prime form satisfy (C.10) among themselves. To verify that the quadratic pieces themselves satisfy the boundary condition, note that for $\Omega(z) = \int_p^z \omega = x(z) + iy(z)$,

$$\partial_t x = \partial_n y = \frac{1}{2}(\partial\Omega + \text{c.c.}) = \frac{1}{2}(\omega/dz + \text{c.c.}) = 0, \quad (\text{C.11})$$

(recall (B.9)) and

$$\partial_t y = \frac{1}{2i}(\partial\Omega - \text{c.c.}) = \partial_n x. \quad (\text{C.12})$$

References

- [1] A. Connes, *Noncommutative Geometry*, Academic Press (1994);
A. Connes and M. Rieffel, in Operator Algebras and Mathematical Physics (Iowa City, Iowa, 1985), pp. 237, *Contemp. Math. Oper. Alg. Math. Phys.* 62, AMS 1987;
A. Connes, M. R. Douglas, and A. Schwarz, *J. High Energy Phys.* **9802:003** (1998), hep-th/9711162.
- [2] M. R. Douglas and C. Hull, *J. High Energy Phys.* **9802:008** (1998), hep-th/9711165.
- [3] M. M. Sheikh-Jabbari, *Phys. Lett.* **B425** (1998) 48, hep-th/9712199; *Phys. Lett.* **B450** (1999) 119, hep-th/9810179.
- [4] Y.-K. E. Cheung and M. Krogh, *Nucl. Phys.* **B528** (1998) 185, hep-th/9803031.
- [5] C.-S. Chu and P.-M. Ho, *Nucl. Phys.* **B550** (1999) 151, hep-th/9812219; hep-th/9906192.
- [6] V. Schomerus, *J. High Energy Phys.* **9906:030** (1999), hep-th/9903205.
- [7] F. Ardalan, H. Arfaei and M. M. Sheikh-Jabbari, hep-th/9803067; *J. High Energy Phys.* **9901:016**, hep-th/9810072; hep-th/9906161.
- [8] N. Seiberg and E. Witten, *J. High Energy Phys.* **9909:032** (1999), hep-th/9908142.
- [9] T. Filk, *Phys. Lett.* **B376** (1996) 53.
- [10] S. Minwalla, M. Van Raamsdonk and N. Seiberg, hep-th/9912072.
- [11] M. Van Raamsdonk and N. Seiberg, hep-th/0002186.
- [12] O. Andreev and H. Dorn, hep-th/0003113.
- [13] Y. Kiem and S. Lee, hep-th/0003145, to appear in *Nucl. Phys.* **B**.
- [14] A. Bilal, C.-S. Chu and R. Russo, hep-th/0003180.
- [15] J. Gomis, M. Kleban, T. Mehen, M. Rangamani and S. Shenker, hep-th/0003215.
- [16] A. Rajaraman and M. Rozali, *J. High Energy Phys.* **0004:033** (2000), hep-th/0003227.
- [17] H. Liu and J. Michelson, hep-th/0004013.
- [18] S. Chaudhuri and E. G. Novak, hep-th/0006014.

- [19] Z. Bern and D. A. Kosower, Nucl. Phys. **B379** (1992) 451.
- [20] K. Roland and H.-T. Sato, Nucl. Phys. **B515** (1998) 488; Nucl. Phys. **B480** (1996) 99.
- [21] A. Frizzo, L. Magnea and R. Russo, Nucl. Phys. **B579** (2000) 379, hep-th/9912183.
- [22] E.S. Fradkin and A. A. Tseytlin, Phys. Lett. **B163** (1985) 123;
 C.G. Callan, C. Lovelace, C. R. Nappi, S.A. Yost, Nucl. Phys. **B288** (1987) 525;
 A. Abouelsaood, C. G. Callan, C.R. Nappi and S.A. Yost, Nucl. Phys. **B280** (1987) 599.
- [23] S.K. Blau, M. Clements, S. Della Pietra, S. Carlip, V. Della Pietra, Nucl. Phys. **B301** (1988) 285.
- [24] M. Bianchi and A. Sagnotti, Phys. Lett. **B211** (1988) 407.
- [25] S. Samuel, Nucl. Phys. **B341** (1990) 513.
- [26] G. Moore, Phys. Lett. **B176** (1986) 369.
- [27] E. Martinec, Nucl. Phys. **B281** (1987) 157.
- [28] C.-S. Chu, R. Russo and S. Sciuto, hep-th/0004183.
- [29] O. Andreev, Phys. Lett. **B481** (2000) 125, hep-th/0001118.
- [30] I. Chepelev and R. Roiban, J. High Energy Phys. **0005:037** (2000), hep-th/9911098.
- [31] W. Fischler, E. Gorbatov, A. Kashani-Poor, S. Paban, P. Pouliot and J. Gomis, J. High Energy Phys. **0005:024** (2000), hep-th/0002067.
- [32] W. Fischler, E. Gorbatov, A. Kashani-Poor, R. McNees, S. Paban, and P. Pouliot, J. High Energy Phys. **0006:032** (2000), hep-th/0003216.
- [33] G. Arcioni, J.L.F. Barbon, J. Gomis, M. A. Vazquez-Mozo, J. High Energy Phys. **0006:038** (2000), hep-th/0004080.
- [34] P. Di Vecchia, F. Pezzella, M. Frau, K. Hornfeck, A. Lerda and S. Sciuto, Nucl. Phys. **B322** (1989) 317.
- [35] S. Hyun, Y. Kiem, S. Lee and C.-Y. Lee, Nucl. Phys. **B569** (2000) 262, hep-th/9909059.
- [36] M. Green, J. Schwarz and E. Witten, *Superstring theory*, Vol. II, Cambridge University Press (1987).